

On Heavy-Quark Free Energies, Entropies, Polyakov Loop, and AdS/QCD

Oleg Andreev*

*Max-Planck Institut für Physik, Föhringer Ring 6, 80805 München, Germany;
L.D. Landau Institute for Theoretical Physics, Kosygina 2, 119334 Moscow, Russia*

Valentin I. Zakharov†

*Istituto Nazionale di Fisica Nucleare – Sezione di Pisa
Dipartimento di Fisica Università di Pisa, Largo Pontecorvo 3, 56127 Pisa, Italy;
Max-Planck Institut für Physik, Föhringer Ring 6, 80805 München, Germany*

Abstract

In this paper we explore some of the features of a heavy quark-antiquark pair at finite temperature using a five-dimensional framework nowadays known as AdS/QCD. We shall show that the resulting behavior is consistent with our qualitative expectations of thermal gauge theory. Some of the results are in good agreement with the lattice data that provides additional evidence for the validity of the proposed model.

PACS: 12.38.Lg, 12.39.Pn, 12.90.+b

1 Introduction

This is our second paper of a series devoted to the thermal properties of a pure gauge theory within a five-dimensional framework nowadays known as AdS/QCD. We explore further the model proposed in the first paper [1]. It is based on the following Euclidean background metric

$$ds^2 = R^2 \frac{h}{z^2} \left(f dt^2 + d\vec{x}^2 + \frac{1}{f} dz^2 \right), \quad h(z) = e^{\frac{1}{2}cz^2}, \quad f(z) = 1 - \left(\frac{z}{z_T} \right)^4, \quad (1.1)$$

where t is a periodic variable of period πz_T such that $z_T = \frac{1}{\pi T}$, with T , the temperature. At zero temperature, we have in fact the slightly deformed AdS₅ metric. Such a deformation is notable because it results in a Regge-like spectrum. This fact allows one to fix the value of c from the ρ meson trajectory. For our purposes, we use the estimate of [2]

$$c \approx 0.9 \text{ GeV}^2. \quad (1.2)$$

*andre@itp.ac.ru

†xxz@mppmu.mpg.de

It is worth noting that the metric (1.1) *does not* contain any free fit parameter. Moreover, the only dimensionful parameter of our model is the Regge slope of meson trajectories. It is quite unusual for QCD, where it is Λ_{QCD} . Thus, evaluations of thermodynamic quantities and the Polyakov loop we are going to undertake can be considered as a further consistency check of our model.

For the case of interest, let us briefly point out a couple of facts.

(i) The free energy of a heavy (static) quark-antiquark pair at finite temperature is expressed in terms of a correlator of two Polyakov loops [3]

$$F(r, T) = -T \ln \langle L(\vec{x}_1) L^\dagger(\vec{x}_2) \rangle + T c(T), \quad (1.3)$$

with $r = |\vec{x}_1 - \vec{x}_2|$ and \vec{x}_i being a point in R^3 . In (1.3) the free energy is defined up to a normalization constant $c(T)$ which is related to the infinite self-energy of the quarks.

There is a subtle point here. In the literature F is often called the heavy quark potential at finite temperature. Apparently, such a definition discards the entropy contribution.¹

An order parameter for the confinement-deconfinement phase transition is the expectation value of the Polyakov loop. After the normalization of (1.3), it is then

$$L = \exp\left\{-\frac{1}{2T} F(r = \infty, T)\right\}. \quad (1.4)$$

(ii) In discussing a Wilson line within AdS/CFT (QCD) [5], one first chooses a contour \mathcal{C} on a four-manifold which is the boundary of a five-dimensional manifold. Next, one has to study fundamental strings on this manifold such that the string world-sheet has \mathcal{C} for its boundary. The expectation value of the loop is schematically given by the world-sheet path integral

$$\langle W(\mathcal{C}) \rangle = \int DX e^{-S_w}, \quad (1.5)$$

where X denotes a set of world-sheet fields. S_w is a world-sheet action.

In principle, the integral can be evaluated semiclassically in terms of minimal surfaces that obey the boundary conditions. The result is written as

$$\langle W(\mathcal{C}) \rangle = \sum_n w_n e^{-S_n}, \quad (1.6)$$

where S_n means a regularized minimal area whose relative weight is w_n .²

The paper is organized as follows. In section 2, we develop the framework we will work. In section 3, we present, on the basis of AdS/QCD, a few results on a heavy quark-antiquark pair in a thermal medium. In particular, we exhibit the free energy, the string tension, and the entropy at low temperatures as well as the Polyakov loop expectation value. We conclude in section 4 with a discussion of some open problems.

¹For a discussion of this issue, see, e.g., [4] and references therein.

²The point is that the areas are divergent but the divergences are proportional to the circumference of \mathcal{C} .

2 General Formalism

Our basic approach will be as follows. It is believed that the correlator of the two Polyakov loops has a path integral representation like that of the Wilson loop.³ Given the background metric, we can attempt to evaluate the values of the regularized areas S_n . If we then discard quantum fluctuations of strings, in the case of one dominant exponent we will get that the free energy is simply proportional to a proper S_*

$$F = TS_*. \quad (2.1)$$

Note that the regularized areas are defined up to normalization constants. Since these constants are in fact due to the infinite self-energy of the quark sources, we omit $c(T)$. Moreover, w_* can be absorbed into a proper normalization constant too. In this paper we will use the approximation (2.1).

But before going on, let us shortly pause here to gain some intuition about the problem at hand. As in [1], we introduce the notion of an effective string tension depending on the fifth coordinate z . It is given by⁴

$$\sigma(z) = \frac{h}{z^2} \sqrt{f(z)}. \quad (2.2)$$

Now consider the behavior of a string bit in the effective potential $V = \sigma(z)$. An important observation is that the form of V is temperature dependent. Indeed, a short algebra shows that there is a special value of temperature $T_1 = \frac{1}{\pi} \sqrt{\frac{c}{27}} \approx 130 \text{ MeV}$.⁵ Below T_1 the effective potential has local extrema at

$$z_{\min} = z_T \sqrt{\frac{2}{\sqrt{3}} \sin\left(\frac{1}{3} \arcsin \frac{T^2}{T_1^2}\right)}, \quad z_{\max} = z_T \sqrt{\frac{2}{\sqrt{3}} \sin\left(\frac{\pi}{3} - \frac{1}{3} \arcsin \frac{T^2}{T_1^2}\right)}, \quad (2.3)$$

while above this temperature the potential is just a decreasing function of z as shown in Fig.1.

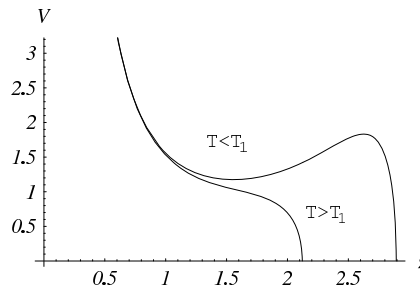


Figure 1: Schematic representation of the effective potential below and above T_1 .

³Note that the corresponding world-sheet has now two boundaries.

⁴It follows from Eq.(2.6).

⁵We use (1.2) for all estimates.

Such a behavior clearly has some of the suspected properties of gauge theory at finite temperature.⁶ For temperatures below T_1 the string ended on the heavy quark-antiquark pair set at $z = 0$ can not get deeper than z_{\min} in z direction because a repulsive force prevents it from doing so. This gives rise somewhat of a wall located at $z = z_{\min}$. The large distance physics of the string is determined by this wall. Since the value of the effective potential (string tension) at its minimum is not vanishing, the quark-antiquark free energy has a dominant linear term whose coefficient is proportional to $\sigma(z_{\min})$. So, this can indeed be interpreted as the low temperature phase. On the other hand, for temperatures above T_1 the string can get deeper and finally reach the horizon $z = z_T$. The large distance physics is now determined by the near horizon geometry. The crucial point is that the effective potential vanishes on the horizon. As a result, there is no linear term in the quark-antiquark free energy. This can be interpreted as the deconfined phase.⁷

Now let us go back to the approach and choose a pair of the contours (Polyakov loops) living on the boundary ($z = 0$) of our five dimensional space. We set

$$\vec{x}_1 = (-\frac{r}{2}, 0, 0), \quad \vec{x}_2 = (\frac{r}{2}, 0, 0). \quad (2.4)$$

Next we want to look for static configurations of the world-sheet action. To this end, we make use of the Nambu-Goto action equipped with the background metric (1.1)

$$S = \frac{1}{2\pi\alpha'} \int d^2\xi \sqrt{\det G_{nm} \partial_\alpha X^n \partial_\beta X^m}. \quad (2.5)$$

There are basically two types of configurations to be considered. One type describes connected surfaces whose boundaries are the Polyakov loops, while another describes disconnected surfaces.

Our first goal will be to analyze connected surfaces. In this case the world-sheet coordinates ξ 's can be chosen as $\xi_1 = t$ and $\xi_2 = x$. With such a choice, the action takes the form

$$S_w = \frac{\mathfrak{g}}{2\pi T} \int_{-\frac{r}{2}}^{\frac{r}{2}} dx \frac{h}{z^2} \sqrt{f + (z')^2}, \quad (2.6)$$

where $\mathfrak{g} = \frac{R^2}{\alpha'}$. A prime denotes a derivative with respect to x .

It is easy to find the equation of motion for z

$$zz'' + (f + (z')^2) (2 - z\partial_z \ln h) - \left(\frac{1}{2}f + (z')^2\right) z\partial_z \ln f = 0 \quad (2.7)$$

as well as its first integral

$$\mathfrak{c} = \frac{hf}{z^2 \sqrt{f + (z')^2}}. \quad (2.8)$$

On symmetry grounds, we have $z'|_{x=0} = 0$. This allows us to express the integration constant \mathfrak{c} via the value of z at $x = 0$. So, we get

$$\mathfrak{c} = \sigma|_{z=z_0}, \quad (2.9)$$

⁶The notion of the effective potential turned out to be useful in studying symmetry breaking (phase transition) within field theories at finite temperature [6]. Like in field theory, our model also has the effective potential whose form is temperature dependent.

⁷Although the above arguments indicate that the phase transition occurs, we should caution the reader that it is a qualitative way of thinking about the problem at hand.

where σ is defined by (2.2) and $z_0 = z|_{x=0}$.

Next we perform the integral over $[-\frac{r}{2}, \frac{r}{2}]$ of dx . By virtue of (2.8), it is given by

$$r = 2 \int_{\mathcal{C}} \frac{dz}{\sqrt{f}} \left(\left(\frac{\sigma}{c} \right)^2 - 1 \right)^{-\frac{1}{2}}, \quad (2.10)$$

where \mathcal{C} is a contour in z plane.

We look for solutions that obey the following condition $z_0 = \max z$. The reason for this is that, on general grounds, the string ended on the quarks set at $x = \pm r/2$ reaches the deepest point in z direction at $x = 0$.

For temperatures below T_1 , there are two possibilities for \mathcal{C} and, as a result, we have

$$r^{(1)} = 2 \int_0^{z_0} \frac{dz}{\sqrt{f}} \left(\left(\frac{\sigma}{c} \right)^2 - 1 \right)^{-\frac{1}{2}}, \quad \text{with } 0 \leq z_0 \leq z_{\min}, \quad (2.11)$$

$$r^{(2)} = 2 \int_{z_{\max}}^{z_0} \frac{dz}{\sqrt{f}} \left(\left(\frac{\sigma}{c} \right)^2 - 1 \right)^{-\frac{1}{2}}, \quad \text{with } z_{\max} \leq z_0 \leq z_T, \quad (2.12)$$

but otherwise r is complex. After a short inspection we find that $r^{(1)}$ is a continuously growing function of z_0 on the interval $[0, z_{\min}]$. Moreover, it equals to zero at $z_0 = 0$ and goes to infinity as $z_0 \rightarrow z_{\min}$. The function $r^{(2)}$ is, unlike $r^{(1)}$, decreasing. It goes from its maximum (finite) value $r_{\max}^{(2)}$ at $z_0 = z_{\max}$ to zero at $z_0 = z_T$ (on the horizon). Thus, the second solution contributes only at distances smaller than $r_{\max}^{(2)}$. To complete the picture, we present the plots of $r^{(i)}$ in Fig.2.

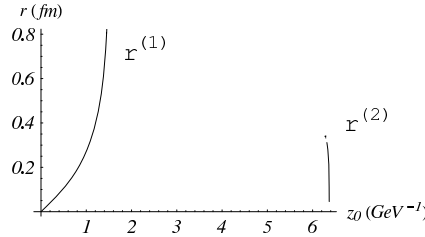


Figure 2: Typical graphs of $r^{(i)}$ below T_1 . Here $T = 0.05$ GeV.

When temperature is increased, the interval $[z_{\min}, z_{\max}]$ becomes smaller and finally disappears at $T = T_1$. For $T > T_1$, a simple analysis leads to the picture that differs noticeably from that of Fig.2. The point is that both the solutions now contribute only at distances smaller than some finite r_{\max} . This is illustrated in Fig.3.

Now we move on to the second type that describes disconnected surfaces. In this case a surface contains two pieces each of which has a topology of a cylinder. The cylinders are stretched from the Polyakov loops on the boundary to the horizon. If we use $\xi_1 = t$ and $\xi_2 = z$ as the world-sheet coordinates, the Nambu-Goto action is then

$$S_w = \frac{g}{2\pi T} \int_0^{z_T} dz \frac{h}{z^2} \sqrt{1 + f(\dot{x})^2}, \quad (2.13)$$

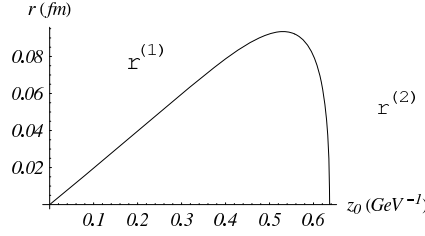


Figure 3: Typical graphs of $r^{(i)}$ above T_1 : $r^{(1)}$ is growing from 0 to r_{\max} , while $r^{(2)}$ is decreasing from r_{\max} to 0. We set $T = 0.5 \text{ GeV}$.

where a dot stands for a derivative with respect to z . The equation of motion for x is

$$\frac{d}{dz} \left(\sigma \dot{x} \left(f^{-1} + (\dot{x})^2 \right)^{-\frac{1}{2}} \right) = 0. \quad (2.14)$$

It is obvious that it has a trivial solution $\vec{x} = \text{const}$ that represents a straight string stretched between the boundary and the horizon. We will call the choice (2.4) the solution $r^{(\infty)}$. Since this solution makes the dominant contribution, as seen from the integrand in (2.13), we will not dwell on other solutions here.

Having discussed the solutions, we can now see what happens with the corresponding areas. We begin with the solution $r^{(1)}$. To this end, we use the first integral to reduce the integral over x to that over z in (2.6). Since the integral is divergent at $z = 0$ due to the factor z^{-2} in the background metric, in the process we regularize it by imposing a cutoff ϵ . At the end of the day, we have

$$S_1^R = \frac{\mathfrak{g}}{\pi T} \int_{\epsilon}^{z_0} \frac{dz}{z^2} h \left(1 - \left(\frac{\mathfrak{c}}{\sigma} \right)^2 \right)^{-\frac{1}{2}}. \quad (2.15)$$

Subtracting the $\frac{1}{\epsilon}$ term we find a finite result

$$S_1 = -\frac{\mathfrak{g}}{\pi T z_0} + \frac{\mathfrak{g}}{\pi T} \int_0^{z_0} \frac{dz}{z^2} \left[h \left(1 - \left(\frac{\mathfrak{c}}{\sigma} \right)^2 \right)^{-\frac{1}{2}} - 1 \right] + \frac{c(T)}{T}, \quad (2.16)$$

where $c(T)$ stands for a normalization constant.

For the second solution $r^{(2)}$, it is a little bit tricky because the minimal surface is built by sewing together two pieces. The first piece comes from $r^{(\infty)}$ defined on the interval $[0, z_{\max}]$. At $z = z_{\max}$, it is sewn with the second piece coming from $r^{(2)}$. The integral (2.13) is divergent at $z = 0$, so we regularize it by imposing the cutoff ϵ as before. After subtracting the divergency, we get

$$S_2 = -\frac{\mathfrak{g}}{\pi T z_{\max}} + \frac{\mathfrak{g}}{\pi T} \int_0^{z_{\max}} \frac{dz}{z^2} (h - 1) + \frac{\mathfrak{g}}{\pi T} \int_{z_{\max}}^{z_0} \frac{dz}{z^2} h \left(1 - \left(\frac{\mathfrak{c}}{\sigma} \right)^2 \right)^{-\frac{1}{2}} + \frac{c(T)}{T}. \quad (2.17)$$

Note that both the areas are regularized in the same way, so the corresponding normalization constants coincide.

For the third solution, the minimal area can be read off from Eq.(2.17). One drops the third term as coming from the solution $r^{(2)}$ and replaces z_{\max} with z_T in the remaining terms. The area is then

$$S_{\infty} = -\mathfrak{g} + \frac{\mathfrak{g}}{\pi T} \int_0^{z_T} \frac{dz}{z^2} (h-1) + \frac{c(T)}{T}. \quad (2.18)$$

Now let us look at the S_i 's as functions of r . We begin with sufficiently low temperature. Since the solution $r^{(2)}$ is defined only for distances smaller than $r_{\max}^{(2)}$, it makes sense to first probe asymptotic behaviors near the point $r = 0$. A short inspection shows that S_1 is not bounded from below, while the others are bounded. This provides a bit of evidence in favor of dominance of S_1 at small distances. Further numerical calculations show that this is indeed the case. Moreover, the first solution turns out to be dominant at physical distances too.⁸ We present the plot of the regularized areas in Fig.4.⁹

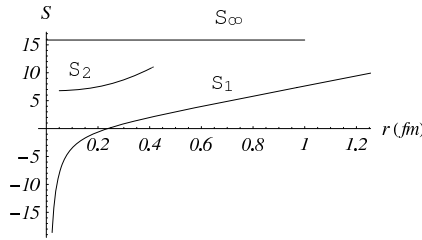


Figure 4: Typical graphs of S_i . Here $T = 0.1$ GeV and $c(T) = 0$.

From this figure it is also clear that there exists a critical distance r_c such that for larger distances S_{∞} becomes dominant. There is an apparent reason for this. At very large distances the quark and the anti-quark decouple from each other. Usually, instability occurs in models with dynamical quarks, where a string breaks. In the case of interest this occurs due to emission of closed strings (glueballs). As known, in AdS/QCD a free particle is described by a straight string stretched between the boundary and the horizon that is nothing but our solution $r^{(\infty)}$.

When temperature is increased, two effects are seen: (1) The minimal difference between the functions S_1 and S_2 becomes smaller. (2) The critical distance r_c is decreasing. For temperatures close to $T = T_1$, S_1 is no longer dominant at physical distances and it is time to account for the other solutions in the series (1.6).

3 Applications

In this section we will consider some applications of the developed formalism. We will focus on the cases where the approximation (2.1) might be applicable.

⁸We mean the interval $0.2 \text{ fm} \lesssim r \lesssim 2 \text{ fm}$ that is of primary importance for phenomenology.

⁹The overall constant \mathfrak{g} can be fixed from the slope of the heavy quark potential at zero temperature. We use the estimate of [8] $\mathfrak{g} \approx 0.94$, here and below.

3.1 Free Energy at Low Temperature

We begin with temperatures which are sufficiently smaller than T_1 . In this case the free energy can be evaluated by using (2.1) with $S_* = S_1$.¹⁰

First, we need to fix the normalization constant $c(T)$. In doing so, we follow [7] and look for the small r expansion of the free energy. Since small distances correspond to small deviations in z direction, we need to study the expressions (2.11) and (2.16) near $z_0 = 0$. The asymptotic behavior of $r(z_0)$ is given by¹¹

$$r = \frac{1}{\rho} z_0 - \frac{c}{4\rho} (1 - \pi\rho^2) z_0^3 + O(z_0^5), \quad (3.1)$$

where $\rho = \Gamma^2(\frac{1}{4})/(2\pi)^{\frac{3}{2}}$.

In a similar way we find the behavior of F . It is

$$F = -\frac{\mathfrak{g}}{2\pi\rho} \frac{1}{z_0} + c(T) + \frac{\mathfrak{g}c}{8\pi\rho} (3\pi\rho^2 - 1) z_0 + O(z_0^3). \quad (3.2)$$

Combining this with (3.1), we get

$$F = -\frac{\kappa_0}{r} + c(T) + \sigma_0 r + O(r^3), \quad (3.3)$$

where $\kappa_0 = \frac{\mathfrak{g}}{2\pi}\rho^{-2}$ and $\sigma_0 = \frac{\mathfrak{g}}{4}c\rho^2$.

Having derived the small distance expansion of the free energy, we can now get that of the singlet free energy¹²

$$F_1 = F - T \ln 9 = -\frac{\kappa_0}{r} + c(T) - T \ln 9 + O(r) \quad (3.4)$$

and compare it with the small distance expansion of the heavy-quark potential at zero temperature. To leading order, we have the same Coulomb term as in [8]. To get an agreement at next-to-leading order, we choose

$$c(T) = T \ln 9 + C. \quad (3.5)$$

Finally, we fix the value of C by matching it to the constant term of the Cornell potential [9]. This yields

$$C = -0.25 \text{ GeV}. \quad (3.6)$$

Actually, our result (3.4) shows that at sufficiently small distances the singlet free energy of the pair is temperature independent. So, the agreement with the lattice data [4, 7] is very satisfactory at this point.

Our next goal is to analyze the long distance behavior of F . As noted in section 2, large r corresponds to $z_0 \sim z_{\min}$. So, we need to study the behavior of (2.11) and (2.16) near $z_0 = z_{\min}$. In this case a crucial observation is that the integrals are dominated by the upper limits, where

¹⁰In the remaining part of this section we omit the index specifying the solution each time when the meaning is clear from the context.

¹¹To this order, the calculation is identical to that of [8].

¹²Here we assume a pure $SU(3)$ gauge theory.

they take the form $\int^1 dv/\sqrt{a(1-v)+b(1-v)^2}$. Such an integral may be found in [10]. At the end of the day, we have

$$r = -w \ln(z_{\min} - z_0) + O(1), \quad F = -\sigma_T w \ln(z_{\min} - z_0) + O(1), \quad (3.7)$$

where $w = 2\sqrt{\sigma/(f\sigma'')}\big|_{z=z_{\min}}$ and $\sigma_T = \frac{g}{2\pi}\sigma\big|_{z=z_{\min}}$.

This means that at long distances the free energy of the pair shows the desired confining behavior

$$F = \sigma_T r + O(1), \quad (3.8)$$

with the string tension

$$\sigma_T = \sigma \frac{e^{t-1}}{t} \left(1 - t^2 \frac{T^4}{T_{\sigma_s}^4}\right)^{\frac{1}{2}}, \quad t = 3 \frac{T_1^2}{T^2} \sin\left(\frac{1}{3} \arcsin \frac{T^2}{T_1^2}\right). \quad (3.9)$$

Here σ denotes a tension at zero temperature. Explicitly, it is given by $\sigma = \frac{g^2}{4\pi}c$ [8]. We have also introduced the critical temperature $T_{\sigma_s} = \frac{1}{\pi}\sqrt{\frac{c}{2}} \approx 210$ MeV obtained from the spatial string tension in [1].

As expected, the string tension σ_T is a decreasing function of T . In Fig.5 we have plotted σ_T/σ against T/T_1 .

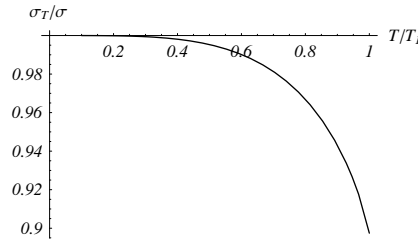


Figure 5: String tension in units of σ versus temperature in units of T_1 .

We conclude this subsection by making a few remarks.

- (i) It is quite interesting that the tension shows *very* little dependence on temperature up to $T \approx 0.8T_1 \approx 100$ MeV.
- (ii) Unlike the coefficient σ_T of the linear term in the large distance expansion of F , the coefficient σ_0 of the linear term in the small distance expansion turns out to be independent of temperature.
- (iii) The free energy of the pair is written in parametric form given by Eqs.(2.11) and (2.16). Since we do not know how to eliminate the parameter z_0 and find F as a function of r , we present the result of numerical calculations. In Fig.6 the free energy F versus r for a temperature below T_1 is shown.

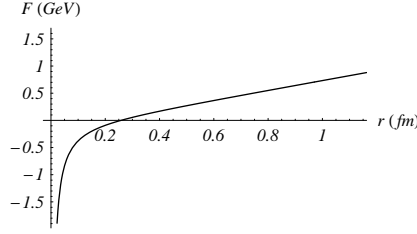


Figure 6: Free energy versus r at $T = 0.1$ GeV.

3.2 Entropy and Energy at Low Temperature

We have already mentioned that in the literature the entropy contributions are sometimes ignored.¹³ It is therefore of great importance to address this issue.

Having understood the behavior of the free energy, we can easily investigate the properties of the entropy. Since the free energy shows no temperature dependence at small distances, it makes sense to focus on long distances, where its behavior is given by (3.8). In this case a straightforward calculation leads to the following expression

$$\mathcal{S} = - \left(\frac{\partial F}{\partial T} \right)_r = - \frac{1}{2} \sigma_T r \left(\frac{\partial \ln f}{\partial T} \right)_{z_{\min}}. \quad (3.10)$$

Here we treat f as a function of two variables. Then, using the relations (1.1) and (2.3), we can compute the entropy density of the pair

$$\frac{\mathcal{S}}{r} = 8 \frac{\sigma_T}{T} \frac{\sin^2 \left(\frac{1}{3} \arcsin \frac{T^2}{T_1^2} \right)}{3 - 4 \sin^2 \left(\frac{1}{3} \arcsin \frac{T^2}{T_1^2} \right)}. \quad (3.11)$$

A closer look at this expression shows that the entropy density grows as the temperature increases. This is the expected result. To complete the picture, we plot the entropy density against T/T_1 in Fig. 7.

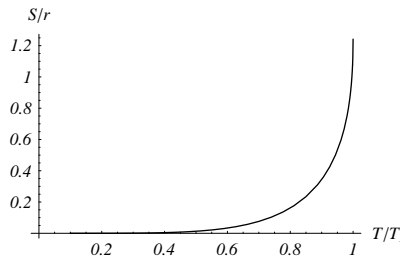


Figure 7: Entropy density versus temperature in units of T_1 .

¹³This is the case for AdS/CFT(QCD) too. See, e.g., [5].

From this figure, we see that the entropy density is close to zero up to temperatures of order $0.4 T_1 \approx 50 \text{ MeV}$. Thus, in this temperature range, the entropy contributions are indeed negligible. It is obvious that the situation changes drastically with the temperature growth. Therefore, a natural question to ask is whether the entropy contributions play a major role at finite temperature. To answer this question, we consider the internal energy of the pair. As usual, it is given by $\mathcal{E} = F + TS$. It is clear from above that \mathcal{E} is independent of temperature at small distances, where it coincides with the heavy-quark potential at zero temperature. At large distances, the internal energy has a complex dependence on temperature together with a linear growth with r . Explicitly, it is given by

$$\mathcal{E} = \Sigma_T r, \quad (3.12)$$

with the tension

$$\Sigma_T = \sigma_T \left(1 + \frac{8 \sin^2 \left(\frac{1}{3} \arcsin \frac{T^2}{T_1^2} \right)}{3 - 4 \sin^2 \left(\frac{1}{3} \arcsin \frac{T^2}{T_1^2} \right)} \right). \quad (3.13)$$

The difference with the string tension (3.9) is due to the second factor that is nothing but the entropy contribution. A direct but lengthy calculation shows that Σ_T is a growing function of temperature. This is in contrast to the behavior of the string tension σ_T discussed in section 3.1. Thus, the entropy contributions *do* play a major role at finite temperature.

We conclude the discussion with a few short comments:

- (i) A temperature growth of the singlet internal energy at large distances was observed in the lattice calculations of [4].
- (ii) The use of thermal AdS as the background metric in the low temperature phase results in zero entropy.¹⁴ This leads to the picture that is completely inconsistent with physics of a pure $SU(3)$ gauge theory at finite temperature.¹⁵
- (iii) In Fig.8 we plot Σ_T versus temperature as provided by the expression (3.13).

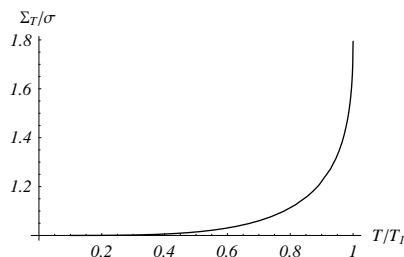


Figure 8: Tension Σ_T in units of σ versus temperature in units of T_1 .

- (iv) It is tempting to see to what extent our predictions for the low temperature behaviors of σ_T and Σ_T are in agreement with the lattice data of [7]. Unfortunately, the lattice data are only

¹⁴In this case $f \equiv 1$, so (3.10) gives zero.

¹⁵Note that the Hawking-Page transition between the thermal AdS space and the Schwarzschild black hole was discussed in [11] as a possible dual description of the deconfinement phase transition for large N_c gauge theories.

available for temperatures close to its critical value.¹⁶

3.3 Polyakov Loop

As noted earlier, at very large separation the quark and anti-quark become free. In this case the dominant exponent is given by S_∞ . So, we are in a situation in which the approximation (2.1) might be applicable. When we use it to find the expectation value of the Polyakov loop, we get

$$L = e^{-\frac{1}{2}S_\infty}, \quad (3.14)$$

with S_∞ the minimal area given by (2.18). Our normalization is stated in (3.5) and (3.6). With this choice, the Polyakov loop expectation value takes the form shown in Fig.9.

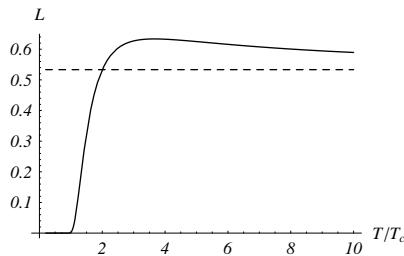


Figure 9: Polyakov loop expectation value versus temperature in units of T_c . The dashed line denotes the value L_∞ .

Certainly, it has the desired behavior: The expectation value of L is zero at low temperatures, while it is nonzero at high temperatures.¹⁷ One sees there is a phase transition from the confined phase to the deconfined phase, as expected. Numerically, the transition temperature is of order

$$T_c \approx 0.11\sqrt{c} \approx 100 \text{ MeV}. \quad (3.15)$$

This is roughly twice smaller than the value found in [1] from the spatial string tension. Thus, the numerical consistency is not good enough at this point.

We chose the normalization constant in the form $c(T) = \alpha T + C$. The meaning of the coefficients is the following: α specifies the value of L at $T = \infty$

$$L_\infty = e^{\frac{1}{2}(\mathfrak{g}-\alpha)}. \quad (3.16)$$

C specifies the form of L . Indeed, the expectation value of the loop is a continuously growing function of temperature for $C \geq 0$, while it has a local maximum for $C < 0$. The position of the maximum is given by a solution to equation

$$CT + \frac{\mathfrak{g}c}{\pi^2} \int_0^1 dx \exp\left\{\frac{1}{2} \frac{cx^2}{\pi^2 T^2}\right\} = 0. \quad (3.17)$$

¹⁶O.A. thanks O. Kaczmarek and P. Petreczky for a discussion of this issue.

¹⁷We consider an absolute value of L .

For our set of parameters a numerical analysis of (3.17) results in $T \approx 3.8 T_c$.

Finally, we can compare the temperature dependence of the Polyakov loop expectation value as provided by our model with the lattice results of [7]. Here there is a subtle point. The lattice data are only available for the range $1.03 \leq \frac{T}{T_c} \leq 6$. This makes it difficult to see what exactly happens in the low temperature phase as well as for high temperatures. We now fix the normalization by fitting (3.14) to the data given in Table 1 of [7] near $T = 6 T_c$. In Fig.10 we have plotted L against $\frac{T}{T_c}$. We find that the temperature dependence is in good agreement for $T \gtrsim 2 T_c$.¹⁸

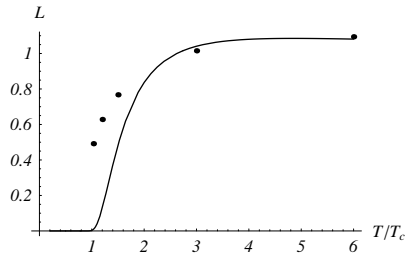


Figure 10: Polyakov loop expectation value versus temperature. Here $c(T) = 0.96 T - 0.18$. The dots denote the data from [7].

4 Discussion

What we have learned is that the 5-dimensional effective model we proposed to study the properties of a heavy quark-antiquark pair at finite temperature turns out to be remarkably consistent with the qualitative expectations of thermal gauge theory. Moreover, in certain cases it provides the analytic results which are in good agreement with the lattice data. It is also worth noting that our model predicts the behavior of the thermodynamic quantities for low temperatures where field theory is unreliable and lattice data are missing.

There are many issues that deserve to be further clarified. Let us mention some of them that are seemed the most important to us.

Apparently, the model suffers from a lack of numerical self-consistency: the value of the critical temperature as seen from the spatial string tension [1] turns out to be at least twice bigger than the value we found from the analysis of the Polyakov loop in section 3.3. There are two lines of thought on this problem.

The first is to account for one-loop corrections in the world-sheet path integral (1.5).¹⁹ This is a complicated problem. Indeed, it is a challenge to theorists to find the world-sheet formulation of string theory on warped geometries like AdS spaces. Among many things, it requires world-sheet fermions and even a world-sheet theta angle that is a two-form field B with an arbitrary value of $\int B$ [12]. But if it was resolved, it could help us to sum the series (1.6) and hence refine the estimates. There is another interesting problem here. What were considered in [13] are some

¹⁸Note that a better agreement is obtained by shifting the plot of Figure 10 a little bit to the left.

¹⁹The model under consideration is an effective theory. It already includes some, but not all, quantum corrections in the approximation we used. The remaining corrections are due to string fluctuations.

low temperature corrections to the string tension. It will be interesting to find similar corrections in our model.

The second line of thought is to somehow modify the background. It may include a slight revision of the metric (1.1) or more radical changes like additional background fields. For instance, a recent proposal of [14] is even to include the tachyon background. If a modification is made, it would produce a number of additional free fit parameters that makes it less attractive for phenomenology. To escape the problem, a clever mechanism for reducing the number of parameters must be invented.

Part of the interest of AdS/CFT(QCD) stems from attempts to understand the physics of RHIC. The reasons are the following: First, a quark-gluon plasma is strongly coupled, so the perturbative QCD is of limited utility. Second, the lattice data do not always provide good information like, for instance on transport properties. On the other hand, AdS/CFT(QCD) offers an alternative way of dealing with this real-world problem.²⁰ It would be particularly interesting to see if our model can shed some light on this subject.

Acknowledgments

O.A. would like to thank O. Kaczmarek, P. Petreczky, M.I. Polikarpov, and E. Shuryak for useful communications and conversations. The work of O.A. was supported in part by Max-Planck-Gesellschaft, Deutsche Forschungsgemeinschaft, and Russian Basic Research Foundation Grant 05-02-16486.

References

- [1] O. Andreev and V.I. Zakharov, The Spatial String Tension, Thermal Phase Transition, and AdS/QCD, hep-ph/0607026.
- [2] O. Andreev, Phys.Rev.D 73, 107901 (2006).
- [3] L.D. McLerran and B. Svetitsky, Phys. Lett.B 98, 195 (1981).
- [4] O. Kaczmarek, F. Karsch, P. Petreczky, and F. Zantow, Nucl.Phys. Proc.Suppl. 129, 560 (2004).
- [5] The literature on the Wilson loops at finite temperature is vast. The following is an incomplete list:
 E. Witten, Adv.Theor.Math.Phys. 2, 505 (1998);
 S.-J. Rey, S. Theisen, and J.-T. Yee, Nucl.Phys.B 527, 171 (1998);
 A. Brandhuber, N. Itzhaki, J. Sonnenschein, and S. Yankielowicz, JHEP 9806, 001 (1998);
 D.J. Gross and H. Ooguri, Phys.Rev.D 58, 106002 (1998);
 H. Dorn and H.J. Otto, JHEP 9809, 021 (1998);
 S.A. Hartnoll and S. P. Kumar, Phys.Rev.D 74, 026001 (2006);
 S.-J. Sin and I. Zahed, Ampere's Law and Energy Loss in AdS/CFT Duality, hep-ph/0606049;
 H. Boschi-Filho, N.R.F. Braga, and C.N. Ferreira, Phys.Rev.D 74, 086001 (2006);
 K. Kajantie, T. Tahkokallio, and J.-T. Yee, Thermodynamics of AdS/QCD, hep-ph/0609254;
 H. Boschi-Filho and N.R.F. Braga, AdS/CFT correspondence and strong interactions, hep-th/0610135.
- [6] D.A. Kirzhnits and A.D. Linde, Phys.Lett.B 42, 471 (1972);
 L. Dolan and R. Jackiw, Phys.Rev.D 9, 3320 (1974);
 S. Weinberg, Phys.Rev.D 9, 3357 (1974).

²⁰For a recent review, see [15].

- [7] O. Kaczmarek, F. Karsch, P. Petreczky, and F. Zantow, Phys.Lett.B 543, 41 (2002).
- [8] O. Andreev and V.I. Zakharov, Phys.Rev.D 74, 025023 (2006).
- [9] E. Eichten, K. Gottfried, T. Konoshita, K.D. Lane, and T.-M. Yan, Phys.Rev.D 17, 3090 (1978); 21, 203 (1980).
- [10] I.S. Gradshteyn and I.M. Ryzhik, Table of Integrals, Series, and Products, Academic Press, 1994.
- [11] E. Witten, as cited in [5];
C.P. Herzog, A Holographic Prediction of the Deconfinement Temperature, hep-th/0608151.
- [12] See the discussion of E. Witten in [5].
- [13] R.D. Pisarski and O. Alvarez, Phys.Rev.D 26, 3735 (1982).
- [14] C. Csaki and M. Reece, Toward a Systematic Holographic QCD: A Braneless Approach, hep-ph/0608266.
- [15] S. Gubser, Relativistic heavy ion collisions and string theory, lectures given at the PiTP 2006 program, [http://www.admin.ias.edu/pitp/2006files/Lecture notes/Gubser Lecture notes REVISED.pdf](http://www.admin.ias.edu/pitp/2006files/Lecture%20notes/Gubser%20Lecture%20notes%20REVISED.pdf).